

Nuclear Symmetry Energy in Terms of Single-Nucleon Potential and Its Effect on the Proton Fraction of β -Stable $npe\mu$ Matter*

Babita Sahoo^{1)**}, Suparna Chakraborty^{2)***}, and Sukadev Sahoo^{3)****}

Received August 24, 2015

Abstract—Momentum and density dependence of single-nucleon potential $u_{\tau}(k, \rho, \beta)$ is analyzed using a density dependent finite range effective interaction of the Yukawa form. Depending on the choice of the strength parameters of exchange interaction, two different trends of the momentum dependence of nuclear symmetry potential are noticed which lead to two opposite types of neutron and proton effective mass splitting. The 2nd-order and 4th-order symmetry energy of isospin asymmetric nuclear matter are expressed analytically in terms of the single-nucleon potential. Two distinct behavior of the density dependence of 2nd-order and 4th-order symmetry energy are observed depending on neutron and proton effective mass splitting. It is also found that the 4th-order symmetry energy has a significant contribution towards the proton fraction of β -stable $npe\mu$ matter at high densities.

DOI: 10.1134/S1063778816010178

1. INTRODUCTION

The nuclear equation of state (EOS) of isospin-asymmetric nuclear matter (ANM) plays a key role for the better understanding of the structure of radioactive nuclei, the reaction dynamics induced by rare isotopes, and the liquid gas phase transition in ANM. It has also got importance due to its implications in certain areas beyond standard nuclear physics, such as astrophysical phenomena like the structure of neutron stars and the dynamics of supernova collisions [1–5]. The equation of state (EOS) of nuclear matter is generally defined as the binding energy per nucleon as a function of density. At zero temperature, the binding energy per nucleon of asymmetric nuclear matter (ANM) can be expressed as a power series of isospin asymmetry $\beta = \frac{\rho_n - \rho_p}{\rho}$, where ρ_n and ρ_p are the neutron and proton densities, respectively, and the total density $\rho = \rho_n + \rho_p$. Up to the 4th-order of the isospin asymmetry β it can be written as [6]

$$E(\rho, \beta) = E(\rho) + E_{\text{sym},2}(\rho)\beta^2 + E_{\text{sym},4}(\rho)\beta^4,$$

where $E(\rho) = E(\rho, \beta = 0)$ represents the binding energy per nucleon of symmetric nuclear matter (SNM), $E_{\text{sym},2}(\rho)$ the 2nd-order nuclear matter symmetry energy, and $E_{\text{sym},4}(\rho)$ the 4th-order nuclear matter symmetry energy. At normal nuclear matter density ρ_0 the 2nd-order symmetry energy $E_{\text{sym},2}(\rho)$ is known to be around 30 MeV from the analysis of nuclear masses within liquid-drop models, the 4th-order symmetry energy $E_{\text{sym},4}(\rho_0)$ has been estimated to be less than 1 MeV [7, 8]. At supra-saturation densities the higher order terms are found to have a significant contribution to the EOS [9]. Unfortunately, we have very limited knowledge about the density dependence of $E_{\text{sym},2}(\rho)$ and $E_{\text{sym},4}(\rho)$. During last few decades significant progress has been made experimentally and theoretically for constraining $E_{\text{sym},2}(\rho)$ around and below normal nuclear matter density [2–5, 10, 11] but at super-normal density its behavior is largely controversial [12–14], whereas the behavior of $E_{\text{sym},4}(\rho)$ is found to be model dependent at these densities [15–21]. Theoretically, almost all many-body theory calculations discussed in the literature so far revealed that the 2nd-order nuclear symmetry energy $E_{\text{sym},2}(\rho)$ positively characterizes the isospin-dependent part of the EOS of ANM and the higher-order terms in the isospin asymmetry are not so important, at least for moderate values of densities [6]. It may be a good approximation to the EOS of ANM, but at the same time it may cause large errors when it is applied to determine some special conditions. For example, the higher order terms in the isospin asymmetry presented in the EOS of ANM

*The text was submitted by the authors in English.

¹⁾Department of Applied Sciences, Durgapur Institute of Advanced Technology & Management, West Bengal, India.

²⁾Department of Physics, Michael Madhusudan Memorial College, West Bengal, Durgapur, India.

³⁾Department of Physics, National Institute of Technology, West Bengal, Durgapur, India.

**E-mail: patra_babita@rediffmail.com

***E-mail: banerjee.suparna@hotmail.com

****E-mail: sukadevsahoo@yahoo.com

at supra-normal densities can significantly modify the proton fraction of neutron stars in β equilibrium [9, 22, 23]. Again, the higher order effects on the incompressibility of ANM have also been studied recently [24, 25]. Therefore possible corrections due to the $E_{\text{sym},4}(\rho)$ term to the EOS of ANM need to be done more accurately. While extracting information about $E_{\text{sym},4}(\rho)$, many transport model simulations have shown that some of the observables in heavy-ion reactions are significantly useful for the study of $E_{\text{sym},4}(\rho)$ in a wide density range. In these transport model simulations of heavy-ion reactions at high and intermediate energies, the EOS enters the reaction dynamics and directly affects the final observables through the single particle potential $u_{\tau}(k, \rho, \beta)$. The single particle potential of a nucleon depends not only on the nuclear density and momentum but also on its isospin, which can be expanded in power series of asymmetry parameter β as in [26].

There are many theoretical models which give the mostly similar description of momentum and density dependence of $u_{\tau}(k, \rho, \beta)$ and $u_{\text{sym},1}(k, \rho)$ around Fermi momentum at saturation and sub-saturation densities, whereas the results significantly differ from each other at high momenta and high densities. From a proper analysis of various theoretical approaches used in the literature so far, it can be ensured that the nonrelativistic finite-range effective interactions, undoubtedly give us a nice platform to simulate the momentum and density dependence of the isoscalar and isovector parts of the nuclear mean field and hence can predict how different properties of nuclear matter are connected to each other. In some of the earlier works [27, 28] the momentum and density dependence of $u_{\tau}(k, \rho, \beta)$ and $u_{\text{sym},1}(k, \rho)$ were analyzed using a simple parameterization of the finite-range effective interactions, which satisfactorily described these quantities at high momenta and high densities. In the present work, we have discussed the existing controversies on two opposite types of neutron and proton effective mass splitting and the extremely divergent nature of nuclear symmetry energy $E_{\text{sym},2}(\rho)$ and $E_{\text{sym},4}(\rho)$ at high densities using a simple density dependent finite range effective interaction. In addition, we also study the effect of nuclear symmetry energy on the proton fraction Y_p of the β -equilibrium $npe\mu$ matter.

This paper is organized as follows. In Section 2 we discuss the formulation of the 1st-order and 2nd-order symmetry potential in ANM. Then we have presented the 2nd-order and 4th-order symmetry energy in terms of the single-nucleon potential. We have also discussed how the momentum dependence of the 1st-order symmetry potential is connected to the momentum dependence of the effective mass as well

as the density dependence of the 2nd-order and 4th-order symmetry energy. The contribution of the 4th-order symmetry energy on the proton fraction Y_p of the β -equilibrium $npe\mu$ matter is also studied. We have presented our conclusions in Section 3.

2. FORMALISM

To study the nuclear EOS and the momentum and density dependence of the single-nucleon potential of ANM we have used a simple density-dependent finite-range effective interaction [28, 29].

$$\begin{aligned} V_{\text{eff}}(r) = & t_0(1 + x_0 P_{\sigma})\delta(r) \quad (1) \\ & + \frac{t_3}{6}(1 + x_3 P_{\sigma}) \left[\frac{\rho(R)}{1 + b\rho(R)} \right]^{\gamma} \delta(r) \\ & + (W + BP_{\sigma} - HP_{\tau} - MP_{\sigma}P_{\tau})f(r), \end{aligned}$$

where $f(r)$ represents a short-range interaction of the conventional form, such as Yukawa, Gaussian, or exponential, and specified by a single range parameter Λ . The other symbols in equation (1) have their usual meanings. This form of effective interaction is very similar to the Skyrme-type of interactions except for the fact that the t_1 and t_2 terms in the latter case have been replaced by the short-range interaction $(W + BP_{\sigma} - HP_{\tau} - MP_{\sigma}P_{\tau})f(r)$. Such a replacement is essential to ensure the description leading to vanishing exchange interaction between a pair of nucleons of very large relative momenta. $P_{\sigma} = \frac{1}{2}(1 + \sigma_1\sigma_2)$ and $P_{\tau} = \frac{1}{2}(1 + \tau_1\tau_2)$ are the spin- and isospin-exchange operators respectively. This simple effective interaction is found to have a zero range density-dependent part similar to skyrme-type interaction and long-range density independent part of conventional form such as Yukawa, Gaussian and Exponential.

The energy density in ANM derived from this effective interaction can be written as

$$\begin{aligned} H(\rho_n, \rho_p) = & \int [f_n(\mathbf{k}) + f_p(\mathbf{k})] \quad (2) \\ & \times (c^2 \hbar^2 k^2 + m^2 c^4)^{1/2} d^3 k \\ & + \frac{1}{2} \left[\frac{E_0^l}{\rho_0} + \frac{E_{\gamma}^l}{\rho_0^{\gamma+1}} \left(\frac{\rho}{1 + b\rho} \right)^{\gamma} \right] (\rho_n^2 + \rho_p^2) \\ & + \left[\frac{E_0^{ul}}{\rho_0} + \frac{E_{\gamma}^{ul}}{\rho_0^{\gamma+1}} \left(\frac{\rho}{1 + b\rho} \right)^{\gamma} \right] \rho_n \rho_p \\ & + \frac{E_{\text{ex}}^l}{2\rho_0} \iint [f_n(\mathbf{k})f_n(\mathbf{k}') + f_p(\mathbf{k})f_p(\mathbf{k}')] \\ & \quad \times g_{\text{ex}}(|\mathbf{k} - \mathbf{k}'|) d^3 k d^3 k' \\ & + \frac{E_{\text{ex}}^{ul}}{2\rho_0} \iint [f_n(\mathbf{k})f_p(\mathbf{k}') + f_p(\mathbf{k})f_n(\mathbf{k}')] \end{aligned}$$

$$\times g_{\text{ex}}(|\mathbf{k} - \mathbf{k}'|)d^3k d^3k',$$

where ρ_n and ρ_p are neutron and proton density, respectively with total nuclear density $\rho = \rho_n + \rho_p$. $f_\tau(\mathbf{k})$ ($\tau = n, p$) are the respective single-particle momentum distribution functions normalized to the local density $\rho_\tau = \int f_\tau(\mathbf{k})d^3\mathbf{k}$.

At zero temperature $f(\mathbf{k})$ is described by a step function $f(\mathbf{k}) = \frac{g}{(2\pi)^3}\theta(k_f - k)$, where g is the spin-

isospin degeneracy factor and $k_f = \left(\frac{3\pi^2}{2}\rho\right)^{\frac{1}{3}}$ is the Fermi momentum. $g_{\text{ex}}(|\mathbf{k} - \mathbf{k}'|)$ is the normalized Fourier transform of the short range interaction $f(r)$ and for the Yukawa form of functional $f(r)$ it is explicitly given as

$$g_{\text{ex}}(|\mathbf{k} - \mathbf{k}'|) = \frac{1}{1 + |\mathbf{k} - \mathbf{k}'|^2/\Lambda^2}.$$

The parameters $E_0^l, E_0^{ul}, E_\gamma^l, E_\gamma^{ul}, E_{\text{ex}}^l, E_{\text{ex}}^{ul}$ are related to the interaction parameters as

$$E_0^l = \rho_0 \left[\frac{t_0}{2}(1 - x_0) \right] \quad (3a)$$

$$+ \left(W + \frac{B}{2} - H - \frac{M}{2} \right) \int f(r)d^3r,$$

$$E_0^{ul} = \rho_0 \left[\frac{t_0}{2}(2 + x_0) + \left(W + \frac{B}{2} \right) \int f(r)d^3r \right], \quad (3b)$$

$$E_\gamma^l = \frac{t_3}{12}\rho_0^{\gamma+1}(1 - x_3), \quad (3c)$$

$$E_\gamma^{ul} = \frac{t_3}{12}\rho_0^{\gamma+1}(2 + x_3), \quad (3d)$$

$$E_{\text{ex}}^l = \rho_0 \left(M - \frac{W}{2} + \frac{H}{2} - B \right) \int f(r)d^3r \quad (3e)$$

and

$$E_{\text{ex}}^{ul} = \rho_0 \left(M + \frac{H}{2} \right) \int f(r)d^3r \quad (3f)$$

The neutron and proton single-particle potential, which is derivable from the energy density, $H(\rho_n, \rho_p)$ can be expressed as

$$u_\tau(k, \rho, \beta) = \left[\left(\frac{E_0^l + E_0^{ul}}{2} \right) \left(\frac{\rho}{\rho_0} \right) \right. \quad (4)$$

$$+ \left(\frac{E_\gamma^l + E_\gamma^{ul}}{2} \right) \frac{(1 + b\rho + \frac{\gamma}{2})}{(1 + b\rho)^{\gamma+1}} \left(\frac{\rho}{\rho_0} \right)^{\gamma+1}$$

$$\left. + \left(\frac{E_{\text{ex}}^l + E_{\text{ex}}^{ul}}{2} \right) \left(\frac{\rho}{\rho_0} \right) I(k, \rho) \right]$$

$$\pm \left[\left(\frac{E_0^l - E_0^{ul}}{2} \right) \left(\frac{\rho}{\rho_0} \right) \right.$$

$$+ \left(\frac{E_\gamma^l - E_\gamma^{ul}}{2} \right) \left(\frac{1}{1 + b\rho} \right)^\gamma \left(\frac{\rho}{\rho_0} \right)^{\gamma+1}$$

$$\left. + \left(\frac{E_{\text{ex}}^l - E_{\text{ex}}^{ul}}{2} \right) \left(\frac{\rho}{\rho_0} \right) I(k, \rho) \right] \beta$$

$$+ \left[\left(\frac{E_\gamma^l - E_\gamma^{ul}}{2} \right) \left(\frac{\gamma}{2} \right) \left(\frac{1}{1 + b\rho} \right)^{\gamma+1} \left(\frac{\rho}{\rho_0} \right)^{\gamma+1} \right] \beta^2$$

for the interaction defined in Eq. (1), where

$$I(k, \rho) = \frac{3\Lambda^2(\Lambda^2 + k_f^2 - k^2)}{8kk_f^3} \quad (5)$$

$$\times In \left[\frac{\Lambda^2 + (k + k_f)^2}{\Lambda^2 + (k - k_f)^2} \right] + \frac{3\Lambda^2}{2k_f^2}$$

$$- \frac{3\Lambda^3}{2k_f^3} \left[\tan^{-1} \left(\frac{k + k_f}{\Lambda} \right) - \tan^{-1} \left(\frac{k - k_f}{\Lambda} \right) \right]$$

for the Yukawa form of interaction.

The +/- before the 2nd square-bracketed term in Eq. (4) is for neutron and proton, respectively.

For the charge symmetry of nuclear interaction under the exchange of neutron and proton, the nuclear single-particle potential or mean field can be expanded in a power series of asymmetry parameter β as [26]:

$$u_\tau(k, \rho, \beta) = u_0(k, \rho) \quad (6)$$

$$\pm u_{\text{sym},1}(k, \rho)\beta + u_{\text{sym},2}(\rho)\beta^2,$$

where $u_0(k, \rho) = u_n(k, \beta = 0, \rho) = u_p(k, \beta = 0, \rho)$ is the single-nucleon potential in SNM, $u_{\text{sym},1}(k, \rho)$ being the well-known nuclear symmetry potential [6] (where $u_{\text{sym},1}$ is denoted by u_{sym}) and the higher order term $u_{\text{sym},2}$ being called as the 2nd-order symmetry potential here.

$$u_0(k, \rho) = u_\tau(k, \rho, \beta)|_{\beta=0} \quad (7)$$

$$= \left(\frac{E_0^l + E_0^{ul}}{2} \right) \left(\frac{\rho}{\rho_0} \right)$$

$$+ \left(\frac{E_\gamma^l + E_\gamma^{ul}}{2} \right) \frac{(1 + b\rho + \frac{\gamma}{2})}{(1 + b\rho)^{\gamma+1}} \left(\frac{\rho}{\rho_0} \right)^{\gamma+1}$$

$$+ \left(\frac{E_{\text{ex}}^l + E_{\text{ex}}^{ul}}{2} \right) \left(\frac{\rho}{\rho_0} \right) I(k, \rho).$$

For the interaction defined in Eq. (1)

$$u_{\text{sym},1}(k, \rho) = \pm \frac{1}{1!} \frac{\delta u_\tau(k, \rho, \beta)}{\delta \beta} \Big|_{\beta=0} \quad (8)$$

$$\begin{aligned}
&= \left(\frac{E_0^l - E_0^{ul}}{2} \right) \left(\frac{\rho}{\rho_0} \right) \\
&+ \left(\frac{E_\gamma^l - E_\gamma^{ul}}{2} \right) \left(\frac{1}{1 + b\rho} \right)^\gamma \left(\frac{\rho}{\rho_0} \right)^{\gamma+1} \\
&+ \left(\frac{E_{\text{ex}}^l - E_{\text{ex}}^{ul}}{2} \right) \left(\frac{\rho}{\rho_0} \right) I(k, \rho), \\
u_{\text{sym},2}(k, \rho) &= \frac{1}{2!} \frac{\delta^2 u_\tau(k, \rho, \beta)}{\delta \beta^2} \Big|_{\beta=0} \quad (9) \\
&= \left(\frac{E_\gamma^l - E_\gamma^{ul}}{2} \right) \left(\frac{\gamma}{2} \right) \left(\frac{1}{1 + b\rho} \right)^{\gamma+1} \left(\frac{\rho}{\rho_0} \right)^{\gamma+1}.
\end{aligned}$$

Neglecting higher order term, equation (6) reduces to Lane potential [30, 31]. But at higher asymmetries these higher order terms cannot be neglected [31].

The complete calculation of neutron and proton mean fields as well as EOS of ANM requires the fixation of nine adjustable parameters, namely, Λ , b , γ , E_0^l , E_0^{ul} , E_γ^l , E_γ^{ul} , E_{ex}^l , and E_{ex}^{ul} . These parameters are constrained on the basis of the information available from the optical model fits to the nucleon-nucleus scattering at intermediate energies, saturation properties of SNM, transport model analysis of flow data heavy-ion (HI) collisions, monopole mode of vibrations in finite nuclei. However, to describe the mean-field properties and the EOS of SNM, only six parameters, namely, Λ , b , γ , E_0 , E_γ and E_{ex} are required. In this context, it may be noted here that the E_0^l , E_0^{ul} , E_γ^l , E_γ^{ul} , E_{ex}^l and E_{ex}^{ul} are related to E_0 , E_γ , E_{ex} as in [28].

The parameters E_{ex} and Λ are determined so as to give the correct momentum dependence of the mean field in SNM at normal nuclear density ρ_0 and at zero temperature as demanded by the optical model fits to nucleon-nucleus scattering data at intermediate energies [32]. The parameter “ b ” appearing in the density-dependent part of the interaction is fixed by requiring the condition that the velocity of sound in nuclear matter at zero temperature should not exceed the velocity of light at high densities. The remaining two strength parameters ($E_0^l + E_0^{ul}$) and ($E_\gamma^l + E_\gamma^{ul}$) can be obtained from the saturation conditions, i.e., (1) Energy per particle $E(\rho_0) = 923$ MeV and (2)

$$\rho \frac{dE(\rho)}{d\rho} \Big|_{\rho=\rho_0} = 0.$$

In this calculation we have considered the standard values of $mc^2 = 939$ MeV and $(c^2 \hbar^2 k_f^2 + m^2 c^4)^{1/2} = 976$ MeV corresponding to $\rho_0 = 0.1658$ fm $^{-3}$. Lastly, the exponent γ is fixed from the value of incompressibility $K(\rho_0) = 210$ MeV. The

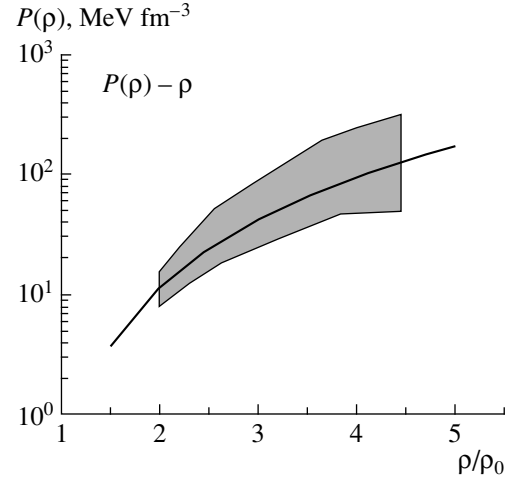


Fig. 1. Pressure–density relation for EOS of SNM at $\gamma = 0.2362$ and compared with the Danielewicz et al. [1] extracted from the flow data in heavy-ion collisions shown by the bounded region.

behavior of SNM around the normal density ρ_0 is determined by energy per particle $E(\rho_0)$ and incompressibility $K(\rho_0)$. Although different theoretical models predict similar values for $E(\rho_0)$, they differ widely in the values of $K(\rho_0)$. Studies on monopole vibrations in finite nuclei using Skyrme-type interactions [33, 34] as well as Gogny-type effective interactions [35] have approximately constrained the value of $K(\rho_0)$ in the range 200–240 MeV. Again, the centroid energies for giant monopole resonances in finite nuclei depend solely on the value of $K(\rho_0)$ [35, 36]. The parameter γ determines the stiffness of the EOS of SNM at high density and can be fixed by using the pressure–density relationship extracted from the analysis of the flow data in high-energy heavy-ion collisions [1] which is presented in Fig. 1 by the bounded region in the density range $2 \leq \rho/\rho_0 \leq 4.6$ (i.e., 0.33 fm $^{-3} \leq \rho \leq 0.762$ fm $^{-3}$). In the same figure the pressure–density curve calculated with the interaction given in Eq. (1) for γ value equaling to 0.2362 corresponding to the incompressibility value $K(\rho_0) = 210$ MeV is also shown. It is clear from Fig. 1 that the results with the interaction given in Eq. (1) compare quite well within the experimentally allowed region.

Once the parameters are fixed by the mean field properties and EOS of SNM, the calculation of neutron and proton mean field properties as well as the EOS of ANM would require the correct splitting of the three parameters like ($E_0^l + E_0^{ul}$), ($E_\gamma^l + E_\gamma^{ul}$) and ($E_{\text{ex}}^l + E_{\text{ex}}^{ul}$) into two specific channels for interactions between like and unlike nucleons. But there are no such experimental/empirical constraints on the splitting of these three combined parameters except for the

value of nuclear symmetry energy $E_{\text{sym}}(\rho_0)$ at normal nuclear matter density from the liquid-drop model. Different choices of these splitting can therefore lead to extremely divergent and even contradicting results on the momentum and density dependence of isovector part of nuclear mean field $u_{\text{sym},1}(k, \rho)$. The value of $u_{\text{sym},1}(k, \rho)$ can be calculated at Fermi momentum k_{f_0} and at normal nuclear matter density ρ_0 for different sets of the parameter of $(E_{\text{ex}}^l + E_{\text{ex}}^{ul})$ for requiring the symmetry energy coefficient $E_{\text{sym},2}(\rho) = 30$ MeV from the empirical liquid-drop mass formula [37, 38], and the nucleon effective mass $\frac{m_0^*}{m}(k_{f_0}, \rho_0) = 0.67$ in SNM. For the Yukawa form of the exchange interaction having the same range but with different strengths (E_{ex}^l) and unlike (E_{ex}^{ul}) nucleons given in set A1 and set A2 $u_{\text{sym},1}(k, \rho)$ is plotted as a function of momentum in Fig. 2.

$$\text{A1) } E_{\text{ex}}^l = \frac{E_{\text{ex}}}{2}, \quad \text{A2) } E_{\text{ex}}^{ul} = \frac{E_{\text{ex}}}{2}.$$

Figure 2 indicates that $u_{\text{sym},1}(k, \rho)$ has a value 26 ± 12 MeV at $k = 0$ and decreases as a function of momentum (k) for the parameter set A1 where E_{ex}^l is greater than E_{ex}^{ul} and increases as a function of k for the parameter set A2, where E_{ex}^{ul} is greater than E_{ex}^l . It needs to be noted here that the momentum dependence of the Lane potential [30], $\nu_1 = 4u_{\text{sym},1}(k = k_{f_0}, \rho_0)$ exhibits a large uncertainty at normal nuclear matter density ρ_0 , as extracted from nucleon–nucleus scattering data and reactions as well as BBG calculations using realistic nucleon–nucleon interactions [30, 39, 40]. Figure 2 also represents that for all the sets of parameters A1 and A2 the value of the Lane potential $\nu_1 = 4u_{\text{sym},1}(k = k_{f_0}, \rho_0)$ lies within the range $\nu_1 = 100 \pm 50$ as quoted in [39]. The values of t_3 , γ , $b\rho_0$, Λ , E_0^l , E_0^{ul} , E_γ^l , E_γ^{ul} , E_{ex}^l and E_{ex}^{ul} for two sets of parameters (specifically, A1 and A2) are given in Table 1.

2.1. 2nd-Order Symmetry Energy in Terms of Nuclear Mean Field in ANM

The 2nd order nuclear symmetry energy $E_{\text{sym},2}(\rho)$ is usually defined by the relation

$$E_{\text{sym},2}(\rho) = \frac{1}{2\rho} \left[\frac{\delta^2 H(\rho_n, \rho_p)}{\delta \beta^2} \right]_{\beta=0}. \quad (10)$$

The behavior of nuclear symmetry energy at sub-saturation density has been studied experimentally and theoretically from the isospin diffusion data in the HI collisions from the NSCL/MSU [2, 41, 42]. Using the isospin- and momentum-dependent

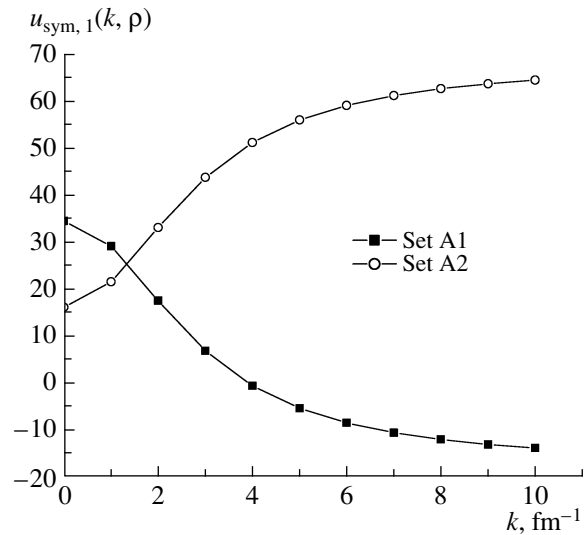


Fig. 2. $u_{\text{sym},1}(k, \rho)$ is plotted as a function of k for parameter sets A1 and A2.

IBUU04 transport model with in medium NN cross sections, the isospin diffusion data were found to be consistent with density dependent symmetry energy of $E_{\text{sym},2}(\rho) \approx 31.6(\rho/\rho_0)^\gamma$ with $\gamma = 0.69-1.05$ at subnormal density [2, 42, 43]. But the high density behavior of 2nd order symmetry energy as predicted by different model calculations [44–47] is extremely divergent and very much contradictory. Basically, it can be classified into two groups [48], first, soft dependence, where the symmetry energy first increases with density, attains a maximum value and then decreases and second, termed as stiff dependence, where the symmetry energy increases monotonically with density. According to the Isospin-dependent Boltzmann Uehling Uhlenbeck (IBUU) transport model [49], the isospin part of mean field $u_{\text{sym},1}(k, \rho)$, gives more complete information than the symmetry energy for the same mean-field approximation at zero temperature. But the momentum and density dependence of the isovector part of the mean field $u_{\text{sym},1}(k, \rho)$ is very much contradictory for different theoretical models. From all these theoretical predictions the momentum dependence of $u_{\text{sym},1}(k, \rho)$ can also be classified into two groups: (i) when $u_{\text{sym},1}(k, \rho)$ increases with momentum, (ii) when $u_{\text{sym},1}(k, \rho)$ decreases with momentum. The density dependence of symmetry energy $E_{\text{sym},2}(\rho)$ can be directly connected to the momentum and density dependence of $u_{\text{sym},1}(k, \rho)$ around Fermi momentum by using Eq. (10),

$$E_{\text{sym},2}(\rho) = \frac{\hbar^2 k_f^2}{6m} \left[\left(\frac{m_0^*(k_f, \rho)}{m} \right)^2 \right] \quad (11)$$

Sets of Interaction Parameters

Set	E_{ex}^l , MeV	E_{ex}^{ul} , MeV	E_{γ}^l , MeV	E_{γ}^{ul} , MeV	E_0^l , MeV	E_0^{ul} , MeV	t_3 , MeV	γ	Λ , fm $^{-1}$	$b\rho_0$
A1	-60.9	-182.7	101.2	202.4	-101.5125	-166.8875	10 975.87	0.2362	2.47	0.0536
A2	-182.7	-60.9	101.2	202.4	-16.08	-252.32				

$$+ \left. \left[\frac{\hbar^2 k_f^2}{m^2 c^2} \right]^{-1/2} + \left[\frac{u_{\text{sym},1}(k, \rho)}{2} - \left(\frac{E_{\text{ex}}^l - E_{\text{ex}}^{ul}}{4} \right) \left(\frac{\rho}{\rho_0} \right) \{I(k, \rho) - I(k_f, \rho)\} \right].$$

Using the above sets of parameters (A1 and A2), $E_{\text{sym},2}(\rho)$ is plotted as a function of ρ in Fig. 3 and is also compared with the experimental result obtained from $E_{\text{sym},2}(\rho) \approx 31.6(\rho/\rho_0)^{0.69}$ [43]. It is found that the experimental result compares quite well with the results obtained from the theoretical calculations using the interaction given in Eq. (1) at low densities. Again, it is observed that for parameter set A1, the 2nd-order symmetry energy $E_{\text{sym},2}(\rho)$ shows soft dependence of density, while for the parameter set A2, the 2nd-order symmetry energy $E_{\text{sym},2}(\rho)$ shows stiff dependence.

The 1st part of Eq. (11) represents the kinetic part of the symmetry energy which shows the effective mass contribution of the SNM and hence shows similar density dependence for all sets of parameters and the 2nd part represents the potential part which is due to the symmetry potential contribution and shows different density dependence for different sets

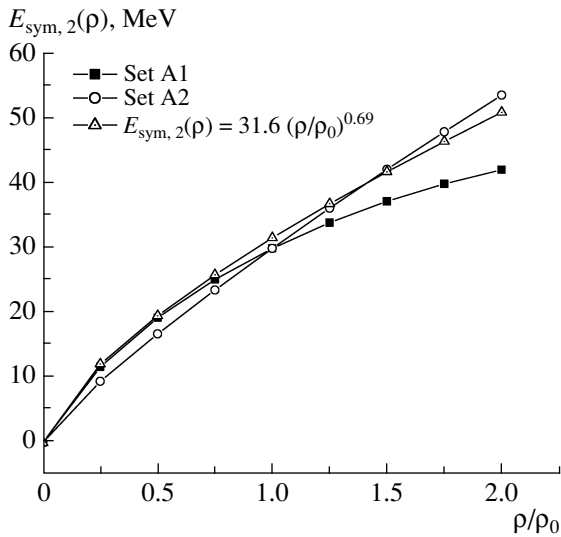


Fig. 3. $E_{\text{sym},2}(\rho)$ is plotted as a function of ρ/ρ_0 for parameter sets A1 and A2 and is compared with the experimental result $E_{\text{sym},2}(\rho) \approx 31.6(\rho/\rho_0)^{0.69}$.

of parameters. Hence, it is clear that the uncertainties observed in the density dependence of the 2nd-order symmetry energy are essentially due to the potential part.

2.2. The 4th-Order Symmetry Energy in Terms of Nuclear Mean Field in ANM

The 4th-order symmetry energy can be obtained by using the relation

$$E_{\text{sym},4}(\rho) = \frac{1}{4! \rho} \left[\frac{\delta^4 H(\rho_n \rho_p)}{\delta \beta^4} \right]_{\beta=0} \quad (12)$$

$$= \frac{\hbar^2 k_f^2}{162m} \left[\left(\frac{m_0^*(k_f, \rho)}{m} \right)^2 + \frac{\hbar^2 k_f^2}{m^2 c^2} \right]^{-1/2}$$

$$+ \frac{1}{648} \left(\frac{E_{\text{ex}}^l + E_{\text{ex}}^{ul}}{2} \right)$$

$$\times [I'''(k_f, \rho) - 6I''(k_f, \rho) + 10I'(k_f, \rho)]$$

$$+ \frac{1}{72} \left(\frac{E_{\text{ex}}^l - E_{\text{ex}}^{ul}}{2} \right) [I''(k_f, \rho) - 2I'(k_f, \rho)],$$

where

$$I'(k_f, \rho) = k \left. \frac{\delta I(k, \rho)}{\delta k} \right|_{k=k_f} \quad I''(k_f, \rho) \quad (13)$$

$$= k^2 \left. \frac{\delta^2 I(k, \rho)}{\delta k^2} \right|_{k=k_f} \quad I'''(k_f, \rho) = k^3 \left. \frac{\delta^3 I(k, \rho)}{\delta k^3} \right|_{k=k_f}.$$

The 1st part of $E_{\text{sym},4}(\rho)$ represents kinetic energy as well as effective-mass contribution, 2nd part arises from the momentum-dependent isoscalar part of the nuclear mean field $u_0(k, \rho)$ and the 3rd part arises from the momentum-dependent isovector part of the nuclear mean field $u_{\text{sym},1}(k, \rho)$. Various contributions to the 4th-order symmetry energies $E_{\text{sym},4}(\rho)$ in different cases are compared in Figs. 4a and 4b. The contributions of kinetic energy part and momentum dependent isoscalar part of the nuclear mean field $u_0(k, \rho)$ part of $E_{\text{sym},4}(\rho)$ are positive and show similar density dependence for all sets of parameters. Isovector part of the nuclear mean field $u_{\text{sym},1}(k, \rho)$ plays the most important role in the determination of high density behaviour of $E_{\text{sym},4}(\rho)$. It shows

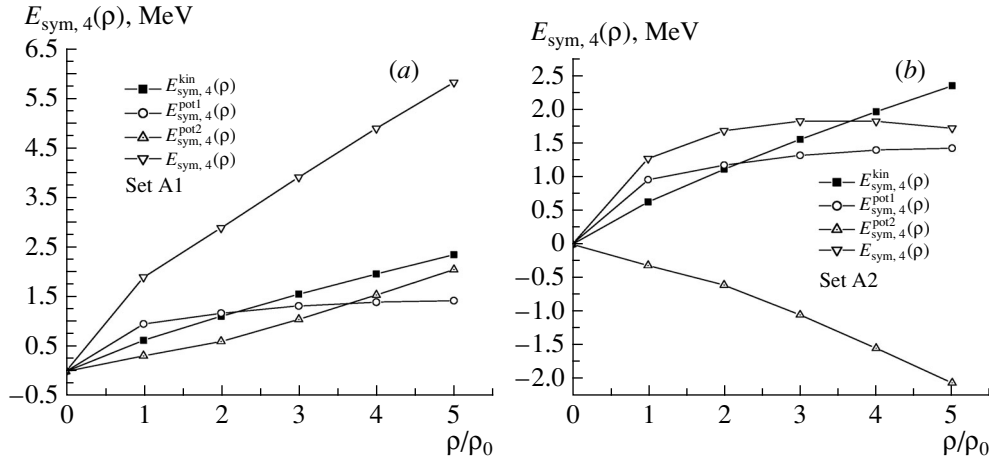


Fig. 4. (a) $E_{\text{sym},4}^{\text{kin}}(\rho)$ and $E_{\text{sym},4}^{\text{pot}}(\rho)$ are plotted as a function of ρ/ρ_0 for parameter set A1. (b) $E_{\text{sym},4}^{\text{kin}}(\rho)$ and $E_{\text{sym},4}^{\text{pot}}(\rho)$ are plotted as a function of ρ/ρ_0 for parameter set A1.

increasing trend with density for the parameters A1 and a decreasing trend for the case of A2.

In order to investigate the effect of higher order symmetry energy $E_{\text{sym},4}(\rho)$ on EOS of ANM, the ratio of 4th-order symmetry energy to 2nd-order symmetry energy, i.e., $\frac{E_{\text{sym},4}(\rho)}{E_{\text{sym},2}(\rho)}$ is calculated. For different sets of parameters A1 and A2 this ratio is plotted as a function of density $\frac{\rho}{\rho_0}$ in Fig. 5. It is found that at normal nuclear matter density ρ_0 this ratio has a very small value about 6% to 7% for parameter set A1 and 3% to 4% for parameter set A2. At high density around $5\rho_0$ it increases up to 13 to 14% for parameter set A1 and decreases up to 1 to 2% for

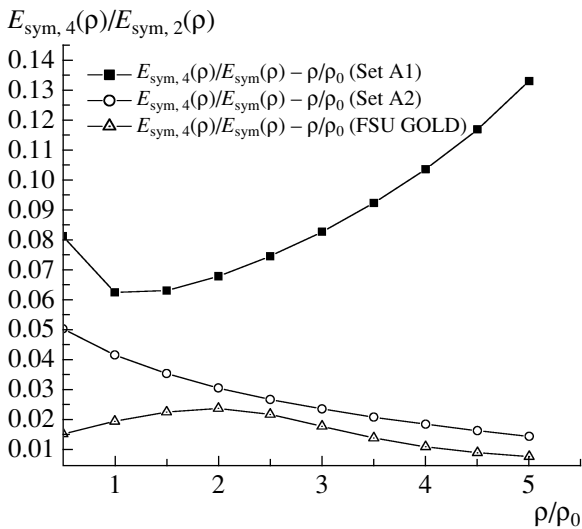


Fig. 5. $E_{\text{sym},4}(\rho)/E_{\text{sym},2}(\rho)$ is plotted as a function of ρ/ρ_0 for parameter set A1, A2 and the result is compared with FSU GOLD model.

parameter set A2. It can be noted here that in low density limit, $\lim_{\rho \rightarrow 0} \frac{E_{\text{sym},4}(\rho)}{E_{\text{sym},2}(\rho)} = 1/27$ as expected from the free Fermi-gas model [9]. In Fig. 5 the ratio $\frac{E_{\text{sym},4}(\rho)}{E_{\text{sym},2}(\rho)}$ for FSU GOLD interaction is also shown for the sake of comparison.

2.3. Contribution of 2nd-Order and 4th-Order Symmetry Energy on Proton Fraction of β -Stable Neutron Star Matter

On the basis of two different splittings of E_{ex}^l and $E_{\text{ex}}^{\text{ul}}$, two different forms of the 2nd-order symmetry energy $E_{\text{sym},2}(\rho)$ and 4th order symmetry energy $E_{\text{sym},4}(\rho)$ have been discussed, from which different predictions on several properties of neutron stars can be studied. To observe the contribution of the 2nd-order and the 4th-order symmetry energy on the EOS of asymmetric nuclear matter, we calculate the proton fraction $Y_p = \frac{\rho_p}{\rho} = \frac{1-\beta}{2}$ in β -stable neutron star matter where the isospin asymmetry β is close to 1. The chemical composition is determined by the requirement of charge neutrality and β equilibrium.

For the β -stable neutron star matter $n \rightarrow p + e^- + \bar{\nu}_e$ and $p + e^- \rightarrow n + \bar{\nu}_e$.

The equilibrium condition requires that the respective chemical potentials satisfy

$$\mu_n = \mu_p + \mu_e + \mu_{\bar{\nu}} \quad (14)$$

and the charge neutrality requires

$$\rho_p = \rho_e = \rho Y_p. \quad (15)$$

The electron density ρ_e in the nonrelativistic limit for noninteracting electron can be denoted as a function of its chemical potential as $\rho_e = \frac{1}{3\pi^2} \mu_e^3$. But neutrinos

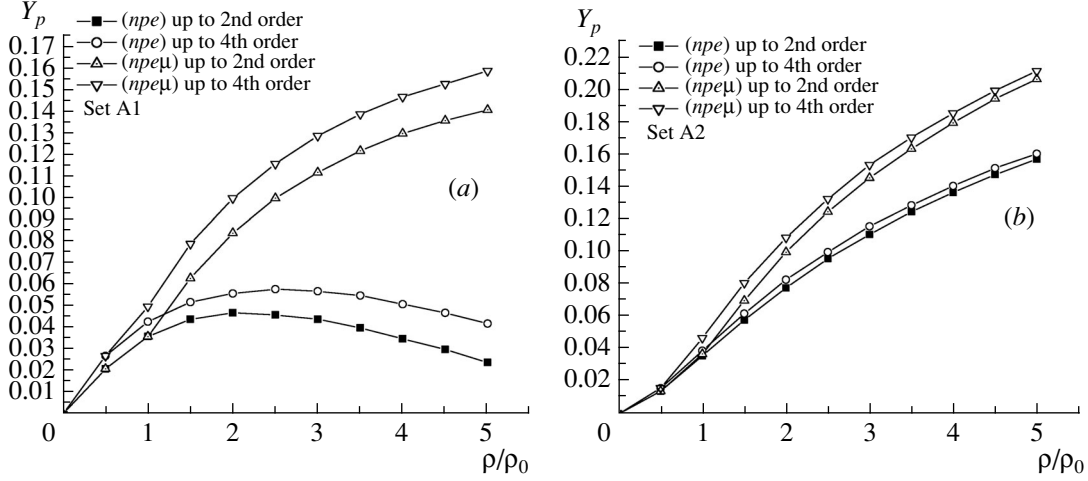


Fig. 6. (a) Proton fraction Y_p for β -equilibrium (npe) and ($npe\mu$) nuclear matter as a function of density up to $E_{\text{sym},2}(\rho)$ and up to $E_{\text{sym},4}(\rho)$ for parameter set A1. (b) Proton fraction Y_p for β -equilibrium (npe) and ($npe\mu$) nuclear matter as a function of density up to $E_{\text{sym},2}(\rho)$ and up to $E_{\text{sym},4}(\rho)$ for parameter set A2.

do not accumulate in neutron stars, hence, few second after their birth $\mu_{\bar{\nu}} = 0$. Below the muon threshold density ($\mu_e < m_\mu c^2 \approx 105.6$ MeV) the charge neutrality condition leads to the following relation [9, 50]

$$\mu_e = \mu_n - \mu_p = 2 \frac{\delta E(\rho, \beta)}{\delta \beta}, \quad (16)$$

$$c\hbar(3\pi^2\rho Y_p)^{\frac{1}{3}} = 4\beta E_{\text{sym},2}(\rho) + 8\beta^3 E_{\text{sym},4}(\rho). \quad (17)$$

As the baryon density exceeds the muon threshold density, where $\mu_e > m_\mu c^2 \approx 105.6$ MeV, the energetic electrons convert to negative muons. In this case the constituents of neutron stars are neutrons, protons, electrons, and muons [51]. The chemical potential equilibrium condition for the ($npe\mu$) system reads

$$\begin{aligned} \mu_e = \mu_\mu = \mu_n - \mu_p \\ = 4\beta E_{\text{sym},2}(\rho) + 8\beta^3 E_{\text{sym},4}(\rho). \end{aligned} \quad (18)$$

The charge neutrality condition is

$$\rho_p = \rho_e + \rho_\mu. \quad (19)$$

The muon density can be expressed as a function of its chemical potential

$$\rho_\mu = \frac{1}{3\pi^2} [\mu_\mu^2 - (m_\mu c)^2]^{3/2} \theta(\mu_\mu - m_\mu), \quad (20)$$

where $\theta(x)$ is the Heaviside step function [51].

The charge neutrality condition can be written as

$$\begin{aligned} 3\pi^2 (c\hbar)^3 \rho Y_p - \mu_\mu^3 \\ - [\mu_\mu^2 - (m_\mu c)^2]^{3/2} \theta(\mu_\mu - m_\mu) = 0, \end{aligned} \quad (21)$$

The equilibrium proton fraction Y_p for (npe) and ($npe\mu$) systems can now be derived by solving Eq. (18) and (21), respectively, considering terms up to $E_{\text{sym},2}(\rho)$ as well as up to $E_{\text{sym},4}(\rho)$. The obtained proton fraction for β -equilibrium (npe) and ($npe\mu$) nuclear matter is plotted as a function of density up to the 2nd-order symmetry energy $E_{\text{sym},2}(\rho)$ and 4th-order symmetry energy $E_{\text{sym},4}(\rho)$ for the above sets of parameters A1 and A2 in Figs. 6a and 6b.

It is found that for all sets of parameters the proton fraction for ($npe\mu$) matter is larger than that for the (npe) nuclear matter. Further it is seen that at high density ($= 5\rho_0$) for the term up to the 4th-order symmetry energy $E_{\text{sym},4}(\rho)$ the proton fraction Y_p for ($npe\mu$) matter increases from 14.1% to 15.9% for set A1, from 20.7% to 21.2% for set A2. These results indicate that the 4th order symmetry energy $E_{\text{sym},4}(\rho)$ may have considerable effects on the proton fraction Y_p in β -stable ($npe\mu$) nuclear matter. In other words, the EOS of asymmetric nuclear matter including the term up to the 4th-order symmetry energy could be a good approximation for the determination of the proton fraction in β -stable ($npe\mu$) nuclear matter.

3. CONCLUSIONS

In this paper we have expressed analytically the 2nd-order and the 4th-order symmetry energy in terms of nuclear mean field in isospin asymmetric nuclear matter using a simple density-dependent finite-range effective interaction having Yukawa form. The density dependence of symmetry potential $u_{\text{sym},1}(k, \rho)$ is studied around Fermi momentum and its role on the 2nd-order and the 4th-order symmetry energy

is observed. The calculations are carried out with the Yukawa form of exchange interaction having the same range but with different strengths for interactions between two like and unlike nucleons, namely set A1 and A2.

Using the derived analytical formula, the 2nd-order symmetry energy is separated into kinetic part and potential part. We have discussed the effective contribution of these two parts towards the 2nd-order symmetry energy parameter for the same density-dependent finite-range effective interaction of Yukawa form. The results so obtained indicate that the kinetic part of the 2nd-order symmetry energy represents the effective mass contribution of symmetric nuclear matter, which is a well-known quantity and it gives the same density dependence for all sets of parameters. The contribution of the potential part is due to the symmetry potential which is not a very well determined quantity and gives different density dependence for different sets of parameters. This indicates that the different density dependence of symmetry energy for different interactions is essentially due to the variation of the symmetry potential.

The density dependence of the 4th-order symmetry energy $E_{\text{sym},4}(\rho)$ is studied for the above sets of parameters A1 and A2. It is found that, for parameter set A1, where E_{ex}^l is greater than E_{ex}^{ul} , the symmetry energy $E_{\text{sym},4}(\rho)$ shows a stiff dependence, while for the parameter set A2, where E_{ex}^{ul} is greater than E_{ex}^l , the symmetry energy $E_{\text{sym},4}(\rho)$ shows a soft dependence of density. The analytical expression of the 4th-order symmetry energy $E_{\text{sym},4}(\rho)$ is also separated into three parts. The 1st part of $E_{\text{sym},4}(\rho)$ represents the kinetic energy as well as effective mass contribution of SNM, 2nd part arises from the momentum-dependent isoscalar part of the nuclear mean field $u_0(k, \rho)$ and the 3rd part arises from the momentum-dependent isovector part of the nuclear mean field $u_{\text{sym},1}(k, \rho)$. The contribution of the kinetic energy part and momentum dependent isoscalar part of the nuclear mean field $u_0(k, \rho)$ part of $E_{\text{sym},4}(\rho)$ are positive and show the similar density dependence for all sets of parameters. The isovector part of the nuclear mean field plays the most important role in the determination of high-density behavior of $E_{\text{sym},4}(\rho)$. It shows an increasing trend with density for parameters A1 and a decreasing trend for the case of A2. It is concluded that different density dependence of the 2nd order as well as the 4th order symmetry energy for different sets of parameters is only due to the variation of $u_{\text{sym},1}(k, \rho)$.

We also investigate the 4th-order $E_{\text{sym},4}(\rho)$ corrections to the EOS of the isospin ANM. Our results indicate that around normal nuclear matter density

the value of $E_{\text{sym},4}(\rho)$ is very small (≈ 1 MeV). At higher densities around $5\rho_0$ it reaches up to 6 MeV to 7 MeV for the parameter sets A1 where the ratio $\frac{E_{\text{sym},4}(\rho)}{E_{\text{sym},2}(\rho)}$ can reach up to 13% to 14% and for the parameter sets A2 it diminishes up to 0.5 MeV to 0.8 MeV and the ratio $\frac{E_{\text{sym},4}(\rho)}{E_{\text{sym},2}(\rho)}$ decreases up to 1% to 2%. These results imply that the effect of the 4th-order symmetry energy $E_{\text{sym},4}(\rho)$ may become non-negligible at higher densities.

Finally we have studied the contribution of the 2nd-order and the 4th-order symmetry energy on the proton fraction of β -stable (npe) and ($npe\mu$) nuclear matter for the above sets of parameters A1 and A2. It is found that for all sets of parameters the proton fraction for ($npe\mu$) matter is larger than that for the (npe) nuclear matter. Further it is seen that at high density ($= 5\rho_0$) for the term up to the 4th-order symmetry energy $E_{\text{sym},4}(\rho)$ the proton fraction Y_p for ($npe\mu$) matter increases from 14.1% to 15.9% for set A1, from 20.7% to 21.2% for set A2. These results indicate that the 4th-order symmetry energy $E_{\text{sym},4}(\rho)$ may have considerable effects on the proton fraction Y_p in β -stable ($npe\mu$) nuclear matter. In other words, the EOS of asymmetric nuclear matter including the term up to the 4th-order symmetry energy could be a good approximation for the determination of the proton fraction in β -stable ($npe\mu$) nuclear matter.

REFERENCES

1. P. Danielewicz, R. Lacey, and W. G. Lynch, Science **298**, 1592 (2002).
2. L.-W. Chen, C. M. Ko, and B.-A. Li, Phys. Rev. Lett. **94**, 032701 (2005).
3. M. B. Tsang et al., Phys. Rev. Lett. **102**, 122701 (2009).
4. M. Centelles, X. Roca-Maza, X. Viñas, and M. Warda, Phys. Rev. Lett. **102**, 122502 (2009).
5. J. B. Natowitz et al., Phys. Rev. Lett. **104**, 202501 (2010).
6. B.-A. Li., L.-W. Chen, and C. M. Ko, Phys. Rept. **464**, 113 (2008).
7. P. J. Siemens, Nucl. Phys. A **141**, 225 (1970).
8. C.-H. Lee, T. T. S. Kuo, G. Q. Li, and G. E. Brown, Phys. Rev. C **57**, 3488 (1998).
9. B.-J. Cai and L.-W. Chen, Phys. Rev. C **85**, 024302 (2012).
10. C. Xu, B.-A. Li, and L. W. Chen, Phys. Rev. C **82**, 054607 (2010).
11. L.-W. Chen, C. M. Ko, and B.-A. Li, Phys. Rev. C **82**, 024321 (2010).
12. Z. Xiao, B.-A. Li, L.-W. Chen, and M. Zhang, Phys. Rev. Lett. **102**, 062502 (2009).
13. Z.-Q. Feng and G. M. Jin, Phys. Lett. B **683**, 140 (2010).
14. C. Xu and B.-A. Li, Phys. Rev. C **81**, 044603 (2010).

15. C. B. Das, S. Das Gupta, C. Gale, and B. A. Li, Phys. Rev. C **67**, 034611 (2003).
16. E. N. E. van Dalen, C. Fuchs, and A. Faessler, Nucl. Phys. A **744**, 227 (2004).
17. S. Fritsch, N. Kaiser, and W. Weise, Nucl. Phys. A **750**, 259 (2005).
18. L.-W. Chen, C. M. Ko, and B.-A. Li, Phys. Rev. C **72**, 064606 (2005).
19. Z.-H. Li, L.-W. Chen, C. M. Ko, et al., Phys. Rev. C **74**, 044613 (2006).
20. R. B. Wiringa et al., Phys. Rev. C **38**, 1010 (1988).
21. M. Kutschera, Phys. Lett. B **340**, 1 (1994).
22. F. S. Zhang and L.-W. Chen, Chin. Phys. Lett. **18**, 142 (2001).
23. A. W. Steiner, Phys. Rev. C **74**, 045808 (2006).
24. L.-W. Chen, B.-J. Cai, C. M. Ko, et al., Phys. Rev. C **80**, 014322 (2009).
25. S. Chakraborty, B. Sahoo, and S. Sahoo, Int. J. Mod. Phys. E **21**, 1250079 (2012).
26. C. Xu, B.-A. Li, L.-W. Chen, and C. M. Ko, Nucl. Phys. A **865**, 1 (2011).
27. S. Chakraborty, B. Sahoo, and S. Sahoo, Nucl. Phys. A **912**, 31 (2013).
28. B. Behera, T. R. Routray, B. Sahoo, and R. K. Satpathy, Nucl. Phys. A **699**, 770 (2002).
29. B. Behera, T. R. Routray, A. Pradhan, et al., Nucl. Phys. A **753**, 367 (2005).
30. A. M. Lane, Nucl. Phys. **35**, 676 (1962).
31. Rong Chen et al., Phys. Rev. C **85**, 024305 (2012) [arXiv: 1112.2936v3 [nucl-th]].
32. B. Behera, T. R. Routray, A. Pradhan, et al., Nucl. Phys. A **794**, 132 (2007).
33. J. P. Blaizot, Phys. Rept. **64**, 171 (1980).
34. B. K. Agrawal and S. Shlomo, Phys. Rev. C **70**, 014308 (2004).
35. J. P. Blaizot, J. F. Berger, J. Decharge, et al., Nucl. Phys. A **591**, 435 (1995).
36. D. H. Youngblood, H. L. Clark, and Y.-W. Kui, Phys. Rev. Lett. **82**, 691 (1999).
37. W. D. Myers and W. J. Swiatecki, Nucl. Phys. A **81**, 1 (1966).
38. K. Pomorski and J. Dudek, Phys. Rev. C **67**, 044316 (2003).
39. K. A. Brueckner and J. Dabrowski, Phys. Rev. **134**, B722 (1964).
40. J. Dabrowski and P. Haensel, Phys. Lett. B **42**, 163 (1972); Phys. Rev. C **7**, 916 (1973).
41. M. B. Tsang et al., Phys. Rev. Lett. **92**, 062701 (2004).
42. B.-A. Li and L.-W. Chen, Phys. Rev. C **72**, 064611 (2005).
43. D. V. Shetty, S. J. Yennello, and G. A. Souliotis, Phys. Rev. C **75**, 034602 (2007).
44. B. A. Li, Nucl. Phys. A **708**, 365 (2002).
45. B. A. Brown, Phys. Rev. Lett. **85**, 5296 (2000).
46. C.-H. Lee, T. T. S. Kuo, G. Q. Li, and G. E. Brown, Phys. Rev. C **57**, 3488 (1998).
47. B. Liu et al., Phys. Rev. C **65**, 045201 (2002).
48. J. R. Stone et al., Phys. Rev. C **68**, 034324 (2003).
49. B. A. Li, Nucl. Phys. A **681**, 434c (2001).
50. I. Bombaci, *Isospin Physics in Heavy-Ion Reactions at Intermediate Energies*, Eds. by B.-A. Li and W. U. Schröder (Nova Science, New York, 2001), p. 35.
51. D. T. Loan, N. H. Tan, D. T. Khoa, and J. Margueron, Phys. Rev. C **83**, 065809 (2011) [arXiv: 1105.5222 [nucl-th]].